



Closed Circuit PRO Series No 5: clean energy generation from seawater and its concentrates by CC-PRO without need of energy recovery

Avi Efraty

Osmotech Ltd, P.O. Box 132, Har Adar 90836, Israel, Tel. +972 52 4765 687; Fax: +972 2 570 0262; email: efraty.adt@012.net.il

Received 17 June 2014; Accepted 3 February 2015

ABSTRACT

This study explores the prospects for clean energy generation in coastal regions from salinity gradient made of seawater (SW) and its concentrates (SWC) by the CC-PRO technology of near absolute energy efficiency without energy recovery device and semi-permeable membranes such as HTI-TFC ($A = 2.49$ lmh/bar, $B = 0.39$ lmh, and $S = 564$ μ m) of 48.3 bar maximum applied pressure and alike. This power generation process is fueled by SW as low salinity feed and SWC as high salinity feed (HSF) and the regeneration of HSF from the produced high salinity diluted feed achieved through evaporation ponds of the types extensively used by the sea salt manufacturing industry. Large-scale harvesting of clean energy from the sea could be found particularly attractive along coastlines of arid zones where climate conditions (e.g. solar radiation, temperature, wind, humidity, etc.) favor effective evaporation from reservoirs of SWC. The simulated CC-PRO process of the SW (4.2%)–SWC (25%) salinity gradient with the HTI-TFC membrane revealed maximum membrane power density of 55.6 W/m² and net electric power density after accounting for the auxiliary pumps of 39.3 W/m² at the hydraulic pressure difference of 48.3 bar under draw/permeation flow ratio of 5.0 and membrane actual/ideal flux ratio of 0.2 estimated from available forward osmosis data of the same membrane in the 1.0–3.0 NaCl salinity gradients range. HTI-TFC membrane surface area of 1,000 m² should provide 943 kWh electric energy per day enough to desalinate 377 m³/d of SW (4.2%) with 50% recovery by means of the closed circuit desalination (CCD) technology (RO: 2.5 kWh/m³). The results of this study reveal that the CC-PRO technology opens the door for large-scale commercial clean power generation from SW–SWC salinity gradients already with existing PRO membranes and improved economic feasibility when PRO membrane of higher actual/ideal flux ratio and burst pressure shall become available in the near future.

Keywords: Forward osmosis (FO); Osmotic power; Salinity gradient power; Pressure-retarded osmosis (PRO); Closed circuit PRO; Evaporation ponds; Seawater; Seawater concentrates; Clean energy generation from seawater

1. Introduction

The rapidly growing global population and standard of living have led to massive combustion of fossil fuels for electric power generation causing a

growing global “green house” effect of adverse climate, environmental, and ecological changes of unfavorable impact on modern life on earth. In many parts on earth, freshwater supplies become scarce, intensity and frequency of storms increased, and arid zones

expanded. The only way to stop the expansion of the global “green house” effect and its adverse impact can be achieved by increased reliance on clean energy sources (e.g. wind, solar, biomass, geothermal, etc.). A newly emerging technology of large-scale clean energy generation prospects is the so-called pressure-retarded osmosis (PRO) method which was conceived by Loeb [1–5] in 1975, the same person which 15 years earlier was the coinventor [6] of reverse osmosis (RO) for seawater and brackish water (BW) desalination. PRO is a membrane technology for hydroelectric power generation from salinity gradients of worldwide abundance such as rivers at their outlets to the sea or of other sources with different concentrations. When two streams of different salinities meet on the opposite sides of a semi-permeable membrane, pressurized water permeation takes place toward the side of higher concentration by a natural forward osmosis (FO) process which in the context of PRO could be used for hydroelectric power generation. The enormous prospects attributed to clean energy generation through PRO are reflected by the rapidly growing activity in this area evident by the increased number of review and review-like articles published [7–20] since 2009 with emphasis on theoretical and experimental studies of advanced PRO membranes [21–32]. Moreover, the PRO concept with an energy recovery device (ERD) was validated by demonstration units in Norway [33–35] and Japan [36–38].

The effective PRO depends on the availability of membranes with high actual/ideal flux ratio (β) of sufficient mechanical strength to withstand the applied pressure of maximum power density as well as on the ability to attain high energy conversion efficiency within the PRO system and it is not yet clear enough whether this is possible with ERD. Noteworthy in this context are the recently reported [39–41] closed circuit PRO (henceforth “CC-PRO”) technology of near absolute energy efficiency without need of ERD and the demonstration of a PRO-TFC membrane with mechanical strength up to 700 psi [32], both important features for the development of viable PRO hydroelectric power generation systems from seawater (SW) and its concentrates (SWC) from evaporation ponds which could be found of high effectiveness especially in arid zones. Salt water constitute ~99% of the global water content and the combination of SW with SWC does not implicate freshwater and/or low salinity BW and/or domestic effluent which could be recycled more efficiently for other applications (e.g. Irrigation, industrial processes, “NEWater”, etc.). Seawater coastlines of arid regions are found anywhere except Europe, although North Africa is short distance from parts of Europe, and could be utilized

effectively for large-scale PRO clean power generation and thereby alleviate the adverse consequences of the global “green-house” effect and its impact on climate and the environment. Arid zones and desert regions are normally characterized by hot dry climate of low rainfall and vast land of little, if any, utility which could be used to create large size evaporation ponds or lakes next to seashores of large SW–SWC salinity gradients for effective PRO hydroelectric power generation even on a gigantic scale. This concept is illustrated schematically in Fig. 1 with SW used as low salinity feed (LSF) and SWC as high salinity feed (HSF) with high salinity diluted feed (HSDF) created during the process converted to HSF (HSDF–HSD) in evaporation ponds by natural renewable solar radiation and wind power. The regeneration of HSF from HSDF involves the evaporation of the permeation volume added to HSF during the process and this implies that identical average flow rates of permeation and evaporation will leave the salinity of the ponds’ systems unchanged. The prevailing climate conditions along coastlines of arid zones and desert regions should make them ideal as preferred sites for the proposed clean energy generation technology.

2. The CC-PRO method

The CC-PRO method [39–41] is illustrated schematically in Fig. 2 with a design comprising four PRO modules with their inlets and outlets connected in parallel to a closed circuit with circulation means (CP) to allow crossflow and two alternately engaged side conduits (SC1 and SC2) with valves means for supply of pressurized HSF to inlets of modules with simultaneous removal of HSDF from their outlets. The pressure in the system is the intrinsically created osmotic pressure of the salinity gradient and the compression

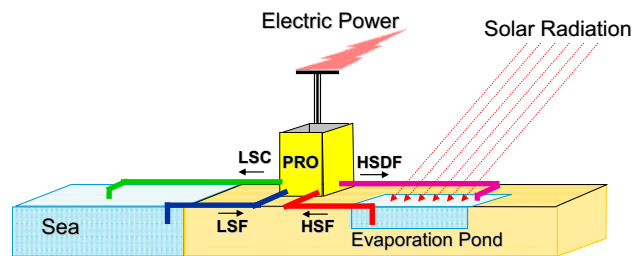


Fig. 1. A schematic illustration of a PRO hydroelectric power generation plant on a desert seashore location with its LSF inlet, low salinity concentrate (LSC) outlet, (HSF or “draw”) inlet from the evaporation pond, and high salinity diluted feed (HSADF or “diluted draw”) outlet to the evaporation pond where the regeneration HSDF–HSF is induced by solar radiation and wind power.

takes account of the various detrimental effects on PRO flux and power generation. Power density curves as function of applied pressure for said salinity gradients consistent with the reported [32] experimental data can be generated by the knowledge of the FO actual/ideal flux ratio (β) for each salinity gradient and the permeability coefficient of HTI-TFC ($A = 2.49$ lmh/bar) by the respective actual flux (J_a —lmh) and power density (W_a — W/m^2) expressions Eqs. (1) and (2) where $\Delta\pi_i$ stands for osmotic pressure difference at module inlet and p for applied pressure. Apart from HTI-TFC, the β - A method for actual power density projections in various salinity gradients also revealed consistent results [45] with the theoretical and experimental power density data reported for the PRO-TFC membranes MP#1 [24], PA-PES [26], PES-A [20], and PES-B [20]. The close resemblance between the power density curves of rigorous theoretical calculations and the β - A method and their agreement with experimental data do suggest the trustworthiness of the β - A power projections. The agreement between β - A power projections and experimental data implies similar detrimental effects on flux in both FO and PRO of strong dependence on the permeability coefficient (A) and module inlet salinity gradient ($\Delta\pi_i$) with footprint of salt diffusion coefficient (B) and structural parameter (S) effects on flux manifested by β .

$$J_a = \beta \times A \times (\Delta\pi_i - p) \quad (1)$$

$$W_a = (1/36) \times J_a \times p = (1/36) \times \beta \times A \times (\Delta\pi_i - p) \times p \quad (2)$$

CC-PRO power projection with HTI-TFC for SW (4.2%)–SWC (25%) require the knowledge of β which can be estimated from the β - A curves of different NaCl gradients furnished in Fig. 3. The osmotic pressure difference of 151.8 bar for SW (4.2%, $\Delta\pi \approx 30.7$ bar)–SWC (25%, $\Delta\pi \approx 182.5$ bar) is about that of 2.5 M NaCl, the average of the 2 and 3 M NaCl in Fig. 3, and implies $\beta \approx 0.157$; however, since the SW–SWC constituents include considerable amounts of divalent anions of distinctly lower reverse salt flux effect, this should effect $\beta \approx 2.00$ value, or higher, for said salinity gradient.

All power density projections for the NaCl gradients to the left of the vertical line at 48.3 bar in Fig. 3 agree with reported experimental data [32], and greater β expected for gradients also containing divalent anions implies higher power densities of 20–30% depending on the concentrations of such anions. The differences between the power projection curves in Fig. 3 as a function of NaCl molar concentrations manifest two opposing effects of increased $\Delta\pi_i$ and

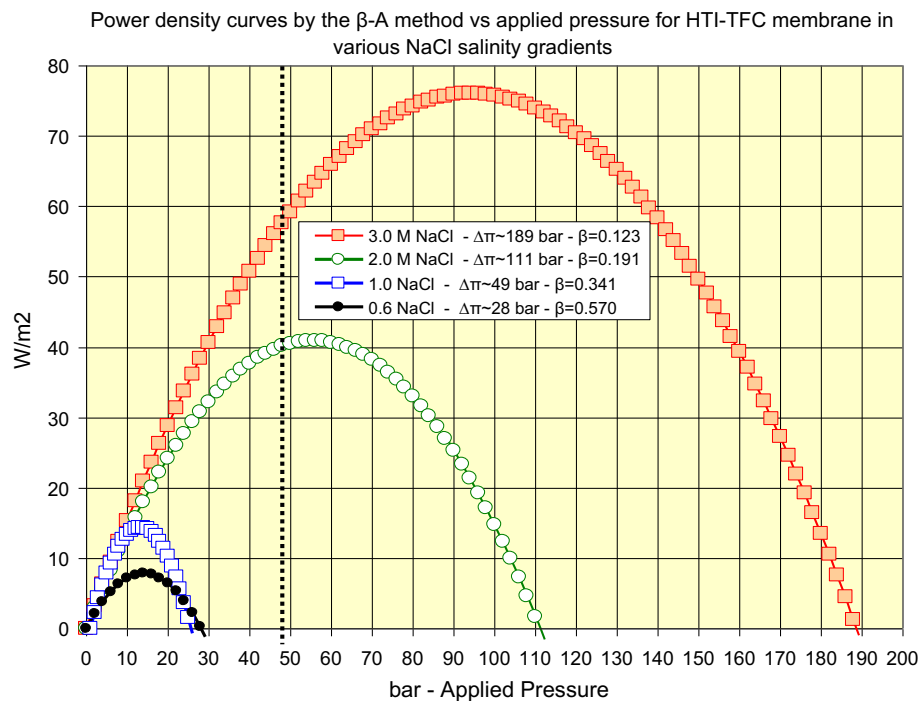


Fig. 3. PRO power density curves by the β - A method for HTI-TFC ($A = 2.49$ lmh) in 0.6, 1.0, 2.0, and 3.0 M NaCl gradients with deionized water with indicated $\Delta\pi_i$ at module inlet and FO actual ideal flux ratio (β) and a vertical line at maximum applied for said membrane (48.3 bar).

declined β with decline moderated in salinity gradient of greater divalent anions compositions.

4. Power prospects from SW (4.2%)–SWC (25%) using CC-PRO with HTI-TFC ($A = 2.49$ lmh/bar and $\beta = 0.200$) in the flow ratio range (δ) 1–25

The theoretical model simulation data base for CC-PRO already disclosed elsewhere [41] is considered hereinafter for SW (4.2%)–SWC (25%) with the HTI-TFC membrane of $A = 2.49$ lmh/bar and $\beta = 0.200$ in the δ range 1–25. The specific data disclosed in Table 1 pertains to the power generation prospects under the stationary state conditions defined by $\delta = 25$ of small concentration difference between HSF at inlet (25.0% - $\Delta\pi_i = 151.6$ bar) and HSDF at outlet (24.0% - $\Delta\pi_o = 134.6$ bar) of the specified module of fixed membrane surface area (42 m²) and intrinsic volume (72.4 L). Noteworthy features in the simulation data base displayed in Table 1 include module inlet, outlet, and average concentrations, osmotic pressures, flux, net driving pressures (NDP), flow rate terms ($Q_{HSF} = Q_{CP}$, Q_p , Q_{LSF} and Q_{LSC}), flow ratio terms

($Q_{CP}/Q_p = Q_{HSF}/Q_p$ and Q_{LSC}/Q_{LSF}), and the power terms of membrane PRO power density (PD), auxiliary pumps consumption, NEP generation after accounting for turbine generator efficiency, and consumption of pumps and the net specific energy (kWh/m³) terms associated with permeation, LSF, and HSF flow components. The efficiency and operational pressure of auxiliary pumps are assumed and the osmotic pressures of the solutions in the process are derived from their concentrations [w/v-%] by the cited $\Delta\pi(\text{bar})/C(\%)$ conversion factor (7.3) which is typical of seawater solutions of same relative composition of constituents. The selected operational pressure difference of CP assumes a module design of low flow friction induced pressure losses. Entry of the selected flow ratio (δ) into the data base in Table 1 generates a complete data-set for the entire applied pressure range and the power data at a specific applied pressure will appear in the table when the selected pressure is entered into the table and the “CC-PRO Selected average Flux” value at the bottom right-hand side of the table adjusted to the value of “ $\Delta\pi$ MOD average” on top. In simple terms, the data displayed in Table 1 are

Table 1
CC-PRO simulation data base with HTI-TFC ($A = 2.49$ lmbar) for the SW (4.2%)–SWC (25%) salinity gradient showing power generation under steady state conditions defined by $\delta = 25$ ($\alpha = 3.85\%$) with $\beta = 0.200$ of PD = 70.9 W/m² and NEP = 28.2 W/m² at 72 bar applied pressure

25.0	% w/v SWC	182.5 bar OP	PRO Membranes Detrimental Effect		Power Demand of CC-PRO PUMPS			
4.20	% w/v SW	30.66 bar OP	0.200	Ratio Actual/Ideal*	Performance	HSP	LSP	CP
		151.8 bar $\Delta\pi$	80.0 % Detrimental Effects		m3/h	37.28	5.96	37.28
Design & Membrane Data			Fixed Flux per Single Module		bar*	0.50	0.50	0.50
1	Number of Modules		35.5	lmh Flux (Selected average)	Efficiency*	0.75	0.75	0.75
1	No of Membrans per Module		1.49	m3/h (Q_p) Module average Permeate	Power (w)	690	110	690
205	cm length of module		24.85	lpm Module average Permeate	TOTAL-Pumps Power Demand (w)	1,491		
30	cm, inner diameter of module		Recycled Flow (CP) of Single Module		TOTAL-Pumps Power Density (W/m2)	35.5		
145	liter, gross volume of module		37.28	m3/h recycling flow (Q_{CP})	Actual PRO only (W/m2)	70.9		
50.0	% membrane volume in module*		621.3	lpm recycling flow (Q_{CP})	Pumps Demand (W/m2)	-35.5		
72.4	liter net volume of Module		0.12	minute complete volume recycle	Turbine-Generator-10% PRO loss	-7.1		
42.0	m2, membrane surface per module		25.00	Selected Flow Ratio (Q_{CP}/Q_p)	Net Electric Power (w/m2)	28.3		
42.0	m2 total surface area of design		0.117 min., HSF residence in module		Energy per m3 Permeation (kWh/m3)	0.798		
LSF-LSC Performance Data			Flow of Entire Design		Energy per m3 LSF (kWh/m3)	0.200		
Module	Unit		1.49	m3/h Permeate Flow of entire unit	Energy per m3 HSF (kWh/m3)	0.032		
5.96	5.96	m3/h LSF Inlet Flow	37.28	m3/h Recycling Flow of entire unit	PRESSURE, NDP and FLUX DATA			
4.20	4.20	% LSF inlet Salinity	3.85 % permeate in HSDF		Permeability Coefficient (l/m2/h/bar)	2.49		
4.47	4.47	m3/h LSC outlet Flow	HSF - HSDF Module Inlet & Outlet Data		Module Parameters	Ideal		Actual
5.60	5.60	% LSC outlet Salinity	25.0	% HSF Module Inlet	Type	NDP	FLUX	FLUX
1.49	1.49	m3/h Permeation Flow	151.8	bar $\Delta\pi$ Module Inlet	Applied -bar	bar	lmh	lmh
4.90	4.90	% mean Salinity (inlet+outlet)/2	24.0	% HSDF Module Outlet	$\Delta\pi$ MOD Inlet	151.8	80	199
35.77	35.77	bar mean $\Delta\pi$ (inlet+outlet)/2	134.6	bar $\Delta\pi$ Module Outlet	$\Delta\pi$ MOD Outlet	134.6	63	156
0.75	0.75	Ratio Q_{LSC}/Q_{LSF} $Q_p=Q_{LSF}-Q_{LSC}$	24.5	% HSDF average	$\Delta\pi$ MOD average	143.2	71.2	177.3
25	25	% permeate from LSF	143.2	bar $\Delta\pi$ Module average	CC-PRO Selected average Flux	35.5		
7.30	$\Delta\pi(\text{bar})/C(\%)$ - HSF at inlet							
7.30	$\Delta\pi(\text{bar})/C(\%)$ - HSDF at outlet							
7.30	$\Delta\pi(\text{bar})/C(\%)$ - LSF & LSC average							

* Assumed

for the stationary state conditions corresponding to $\delta = 25$ at a specific applied pressure of 72 bar under which $PD = 70.9 \text{ W/m}^2$ and $NEP = 28.3 \text{ W/m}^2$.

The PD of CC-PRO with HTI-TFC ($A = 2.49 \text{ lmh}$) and $\beta = 0.200$ for SW (4.2%)–SWC (25%) as function applied pressure and flow ratio ($FR = \delta$) displayed in Fig. 4 shows peak applied pressure drift (52–92 bar) of maximum power change ($35.3\text{--}65.2 \text{ W/m}^2$) inversely proportional to δ (1–25) with vertical dotted line indicating the limiting pressure of HTI-TFC. The power information disclosed in Fig. 5(A) and (B) is of the same nature as in Fig. 4 but with respect to NEP, the most important product of the CC-PRO technology. The peak applied pressure drift of maximum NEP in Fig. 5(A) shows declined pressure (92–76 bar) with increased PD ($46.2\text{--}33.2 \text{ W/m}^2$) associated with decreased δ (25–7.5). The peak applied pressure drift of maximum NEP in Fig. 5(B) shows declined pressure (70–58 bar) associated with decreased PD ($45.7\text{--}29.1 \text{ W/m}^2$) and δ (5.0–1.0). Maximum NEP availability of $45.7\text{--}46.2 \text{ W/m}^2$ in the gradient system under review corresponds to the peak pressure range 70–76 bar of stationary state conditions defined by δ of 5.0–7.5, respectively. Noteworthy features in Figs. 4 and 5(A)–(B) relate to the difference between peak pressures associated with maximum PD and NEP with the latter NEP taking place with applied

pressures not too far removed from the membrane limit (48.3 bar) and thereby suggesting the plausibility of CC-PRO with HTI-TFC for SW (4.2%)–SWC (25%) already at the current state of the art.

The power generation prospects from SW (4.2%)–SWC (25%) with CC-PRO and HTI-TFC ($A = 2.49 \text{ lmh/bar}$) of actual/ideal flux ratio $\beta = 0.200$ are summarized in Table 2(A) and (B) as a function of flow ratio (δ) and of peak applied pressure [A], or at 48.3 bar [B]. Other noteworthy information provided in this table pertains to specific energy (kWh/m^3) associated with permeation, LSF, and HSF as well as NEP generation per $1,000 \text{ m}^2$ surface area of membranes and its translation to daily clean energy output (kWh/d) and daily desalinated volume of seawater (m^3/d) by the SWRO-CCD technology [46–48] ($4.2\text{--}2.5 \text{ kWh/m}^3$). The high NEP generation prospects in the system under review of $45.7\text{--}45.3 \text{ W/m}^2$ correspond to the respective ranges of flow ratio (δ : 5.0–10) and applied pressure (70–80 bar) with maximum of 46.2 W/m^2 attained at 76 bar with $\delta = 7.5$. The performance data of the system under review at the pressure limitation (48.3 bar) of the HTI-TFC membrane in Table 2(B) reveal a maximum NEP of 39.3 W/m^2 at $\delta = 5.0$, or approximately 85% of the best NEP availability in this system (46.2 W/m^2 ; $\delta = 7.5$; 76 bar).

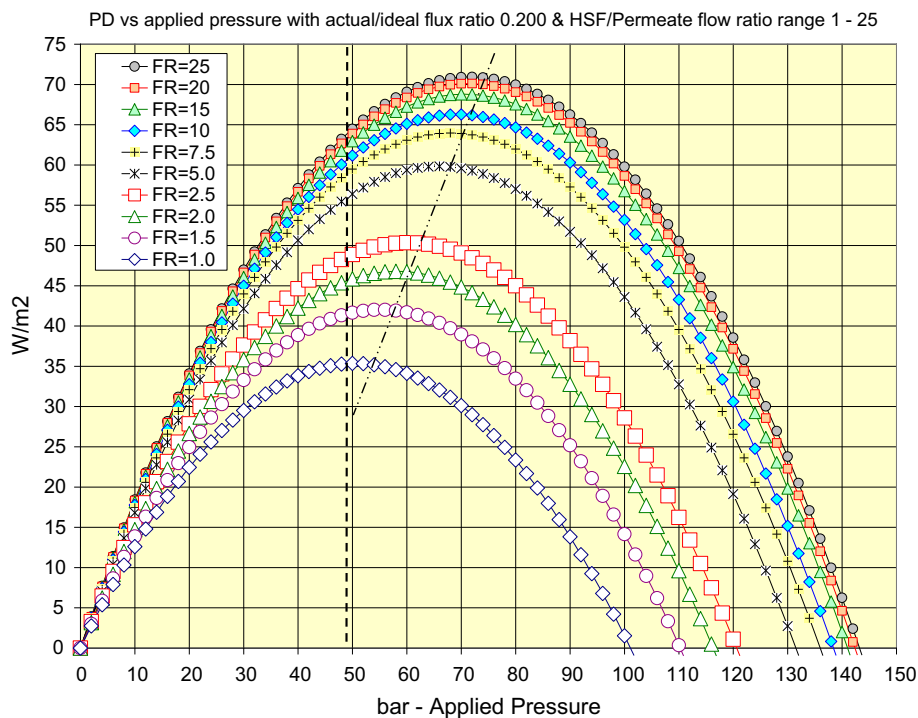


Fig. 4. PD as function of applied pressure and flow ratio (δ : 1–25) for SW (4.2%)–SWC (25%) using CC-PRO with HTI-TFC ($A = 2.49 \text{ lmh}$) and $\beta = 0.200$ showing peak pressure drift of maximum power as function of δ with vertical dotted line indicating the limiting pressure HTI-TFC.

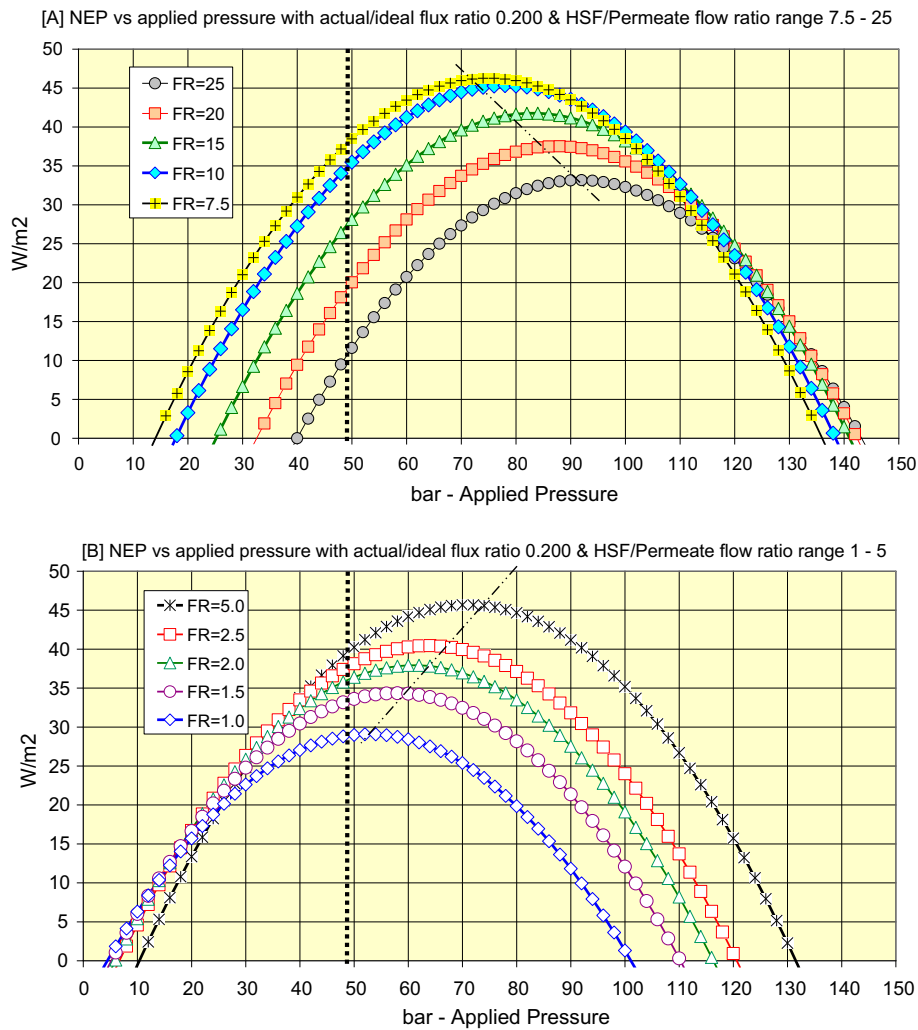


Fig. 5. NEP as function of applied pressure and flow ratio (δ) for SW (4.2%)–SWC (25%) using CC-PRO with HTI-TFC ($A = 2.49$ lmh) and $\beta = 0.200$ for δ ranges 1–5 [A] and 7.5–25 [B] showing peak pressure drift of maximum power as function of δ with vertical dotted line indicating the limiting pressure of HTI-TFC.

PD and NEP variations, respectively, as function applied pressure and flow ratio (δ) according to Table 2(A) are displayed in Fig. 6 and NEP specific energy variations as function flow ratio in Fig. 7(A) and applied pressure in Fig. 7(B). PD and NEP as function of flow ratio (δ) at 48.3 bar applied pressure according to the data in Table 2(B) are displayed in Fig. 8(A) and (B).

5. Maximum power generation prospects from SW (4.2%)–SWC (25%) using CC-PRO with HTI-TFC ($A = 2.49$ lmh/bar) under $\delta = 5.0$ at 48.3 bar applied pressure (48.3 bar) in the actual/ideal flux ratio (β) range 0.18–0.27

The actual/ideal flux ratio ($\beta = 0.200$) used for CC-PRO and HTI-TFC power simulation of SW (4.2%)–

SWC (25%) according to the database in Table 1 is suggested by the β - A method as a reasonable choice and the dependence of power generation on β (range: 0.18–0.27) is exemplified in Table 3 and Fig. 9 under the conditions of $\delta = 5.0$ and 48.3 bar applied pressure of maximum NEP availability according to Table 2(B). The plausible β range of 0.200–0.23 for the system under review corresponds to maximum NEP density of 39.3–43.2 W/m² and daily clean energy output of 943–1,037 kWh per 1,000 m² of membrane surface, respectively. The small uncertainty with respect to the true value of β arises from its extrapolation on the basis of NaCl solutions instead of seawater concentrates where reverse salt diffusion is lower due to the presence of divalent ions. The NEP projections of 39.3–43.2 W/m² for SW (4.2%)–SWC (25%) with CC-PRO and HTI-TFC at 48.3 bar suggest the

Table 2

Power generation prospects from SW (4.2%)–SWC (25%) using CC-PRO and HTI-TFC ($A = 2.49$ lmh/bar) with actual/ideal flux ratio $\beta = 0.200$ as function of flow ratio (δ) and of peak applied pressure (A) as well as at 48.3 bar (B) according to the simulation data base in Table 1 under the conditions defined by A , β , δ , and the applied pressure—maximum power columns labeled bold

HSF/Permeate flow ratio, δ	25	20	15	10.0	7.5	5.0	2.5	2.0	1.5	1.0
Percent permeate in HSDF, α	3.85	4.76	6.25	9.09	11.76	16.67	28.57	33.33	40.00	50.00
(A) Peak pressure prospects										
Membrane power density (W/m^2)	65.2	66.2	66.3	65.2	63.1	59.6	50.2	46.6	41.9	35.3
Net electric power (NEP) Density (W/m^2)	33.2	37.5	41.8	45.3	46.2	45.7	40.4	37.9	34.3	29.1
Net electric power (NEP) per module (kW)*	1.394	1.575	1.756	1.903	1.940	1.919	1.697	1.592	1.441	1.222
Energy per m^3 permeation (kWh/m^3)	1.301	1.384	1.47	1.505	1.547	1.493	1.443	1.405	1.321	1.186
Energy per m^3 LSF (kWh/m^3)	0.325	0.346	0.368	0.375	0.387	0.373	0.359	0.351	0.330	0.297
Energy per m^3 HSF (kWh/m^3)	0.052	0.069	0.098	0.151	0.206	0.299	0.574	0.702	0.881	1.186
Peak applied pressure (bar)	92	88	84	80	76	70	64	62	58	52
NEP per 1000 m^2 membrane (KW)	33.2	37.5	41.8	45.3	46.2	45.7	40.4	37.9	34.3	29.1
Daily energy per 1,000 m^2 membrane (kWh/d)	797	900	1,003	1,087	1,109	1,097	970	910	823	698
Desalinated SW (4.2%—2.5 kWh/m^3) equivalent (m^3/d)	319	360	401	435	444	439	388	364	329	279
(B) Prospects at 48.3 bar applied pressure										
Membrane power density (W/m^2)	63.4	62.9	62.0	60.2	58.6	55.6	48.3	45.4	41.4	35.3
Net electric power (MEP) density (W/m^2)	9.8	18.4	26.7	34.2	37.4	39.3	37.5	35.9	33.2	28.8
Net electric power (NEP) per module (kW)*	0.412	0.773	1.121	1.436	1.571	1.651	1.575	1.508	1.394	1.210
Energy per m^3 permeation (kWh/m^3)	0.207	0.394	0.577	0.763	0.855	0.950	1.042	1.058	1.079	1.096
Energy per m^3 LSF (kWh/m^3)	0.052	0.098	0.144	0.191	0.214	0.237	0.260	0.265	0.270	0.274
Energy per m^3 HSF (kWh/m^3)	0.008	0.020	0.038	0.076	0.114	0.190	0.417	0.529	0.717	1.096
NEP per 1000 m^2 membrane (KW)	9.8	18.4	26.7	34.2	37.4	39.3	37.5	35.9	33.2	28.8
Daily energy per 1000 m^2 membrane (kWh/d)	235	442	641	821	898	943	900	862	797	691
Desalinated SW (4.2%—2.5 kWh/m^3) equivalent (m^3/d)	94	177	256	328	359	377	360	345	319	276

*Single module of 42 m^2 membrane surface.

economic feasibility of this clean power generation technology for immediate application at the current state of the art. Improved membranes of high β (>0.200) and operational pressure (>48.2 bar) expected in the near future will make this approach of SW–SWC useful for clean energy generation even more attractive.

6. Discussion

This study examines the prospective application of CC-PRO for hydroelectric power generation from a model salinity gradient made of SW (4.2%)–SWC (25%) with the HTI-TFC membrane of the highest reported [32] operational pressure (48.3 bar). Performance analysis of the process under review utilizes the CC-PRO simulation data base in Table 1 which takes account of modules' inlet (HSF and LSF) and outlet (HSDF and LSC) concentrations; flow rates of HSF, HSDF, LSF, and LSC; flow ratio of LSC/LSF and of HSF/permeation (δ) which defines the stationary state conditions

inside PRO the modules; actual/ideal flux ratio (β) which together with the permeability coefficient (A) defines the performance characteristics of the membrane; power requirements of auxiliary pumps; efficiency of the turbine generator system; and other pertinent information for PRO power projections. The β factor in Table 1 is the estimated FO actual/ideal flux ratio for the HTI-TFC membrane on the basis of reported [32] experimental data in various NaCl solutions according to the procedure described elsewhere in this article, with correction for the presence divalent ions in seawater. Summary of the simulated model system analysis with emphasis on power aspects appears in Table 2(A) with data correlation to flow ratio (δ) and applied pressure in Figs. 6 and 7. The difference between PD and NEP is evident from their respective curves in Fig. 6 as function of flow ratio (δ) and applied pressure with maximum PD ($66.3 W/m^2$) attained at $\delta = 15$ and 84 bar; whereas, maximum NEP ($46.2 W/m^2$) is reached at $\delta = 7.5$ and 76 bar applied pressure. Distinction between PD and NEP is rather

Table 3

Clean power generation prospects from SW (4.2%)–SWC (25%) with CC-PRO and HTI-TFC ($A = 2.49$ lmh/bar) at its maximum operational pressure (48.3 bar) under module stationary state conditions of maximum NEP ($\delta = 5.0$ and $\alpha = 16.67\%$) in the actual/ideal flux ratio (β) range 0.18–0.27 according to the simulation database in Table 1—bold column stands for $\beta = 0.200$.

Percent permeate in HSDF, α	5.0	5.0	5.0	5.0	5.0	5.0	5.0	5.0	5.0	5.0
Actual/Ideal flux ratio, β	0.18	0.19	0.20	0.21	0.22	0.23	0.24	0.25	0.26	0.27
Prospects at 48.3 bar applied pressure as function actual/ideal flux ratio										
Membrane power density (W/m^2)	50.0	52.8	55.6	58.4	61.2	63.9	66.7	69.5	72.3	75.1
Net electric power density (W/m^2)	35.4	37.3	39.3	41.3	43.2	45.2	47.2	49.1	51.1	53.1
Net electric power per single module (kW)*	1.487	1.567	1.651	1.735	1.814	1.898	1.982	2.062	2.146	2.230
Energy per m^3 permeation (kWh/m^3)	0.949	0.949	0.949	0.949	0.949	0.949	0.949	0.949	0.949	0.949
Energy per m^3 LSF (kWh/m^3)	0.237	0.237	0.237	0.237	0.237	0.237	0.237	0.237	0.237	0.237
Energy per m^3 HSF (kWh/m^3)	0.190	0.190	0.190	0.190	0.190	0.190	0.190	0.190	0.190	0.190
NEP per 1,000 m^2 membrane (KW)	35.4	37.3	39.3	41.3	43.2	45.2	47.2	49.1	51.1	53.1
Daily energy per 1,000 m^2 membrane (kWh/d)	850	895	943	991	1,037	1,085	1,133	1,178	1,226	1,274
Desalinated SW (4.2%–2.5 kWh/m^3) equivalent (m^3/d)	340	358	377	396	415	434	453	471	491	510

*Single module 42 m^2 membrane surface.

important since the economic feasibility of PRO is determined by the latter, the energy sold to clients. The specific energy (kWh/m^3) terms in Table 2(A) express the amount of net PRO energy (kWh) per unit volume (m^3) of feed solutions (LSF and HSF) and permeation with correlation to flow ratio displayed in Fig. 7(A) and to applied pressure in Fig. 7(B). The

information disclosed in Figs. 6 and 7 reveals the flow ratio and applied pressure conditions of maximum PD and NEP with its specific energy components.

The performance characteristics of the HTI-TFC membrane in the context of CC-PRO and the SW (4.2%)–SWC (25%) model system in Table 2(A) and Figs. 6 and 7 ignores the pressure limitation (48.3 bar)

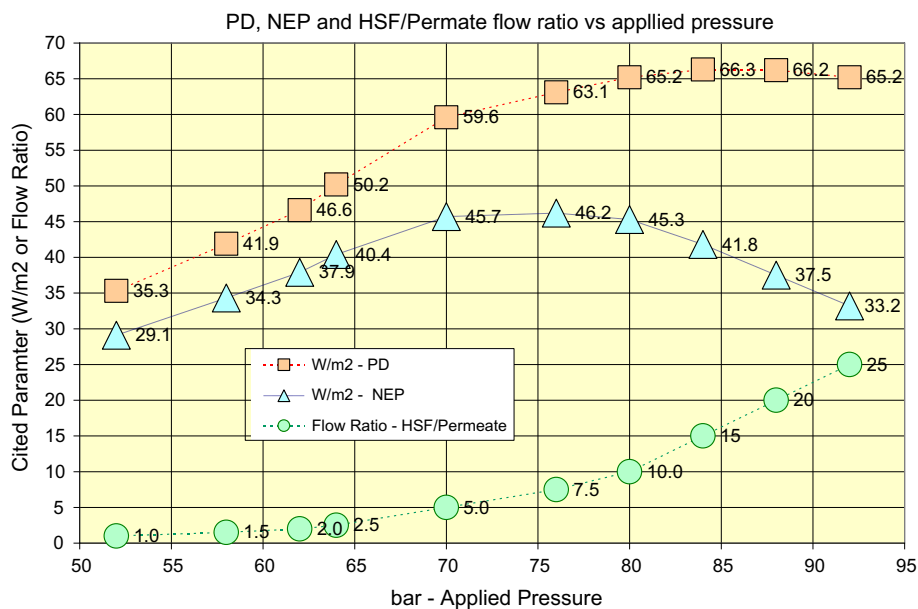


Fig. 6. Power generation (PD and NEP) prospects from SW (4.2%)–SWC (25%) using CC-PRO with HTI-TFC ($A = 2.49$ lmh) and $\beta = 0.200$ as function of applied pressure and flow ratio (δ) which defines the stationary state conditions of operation.

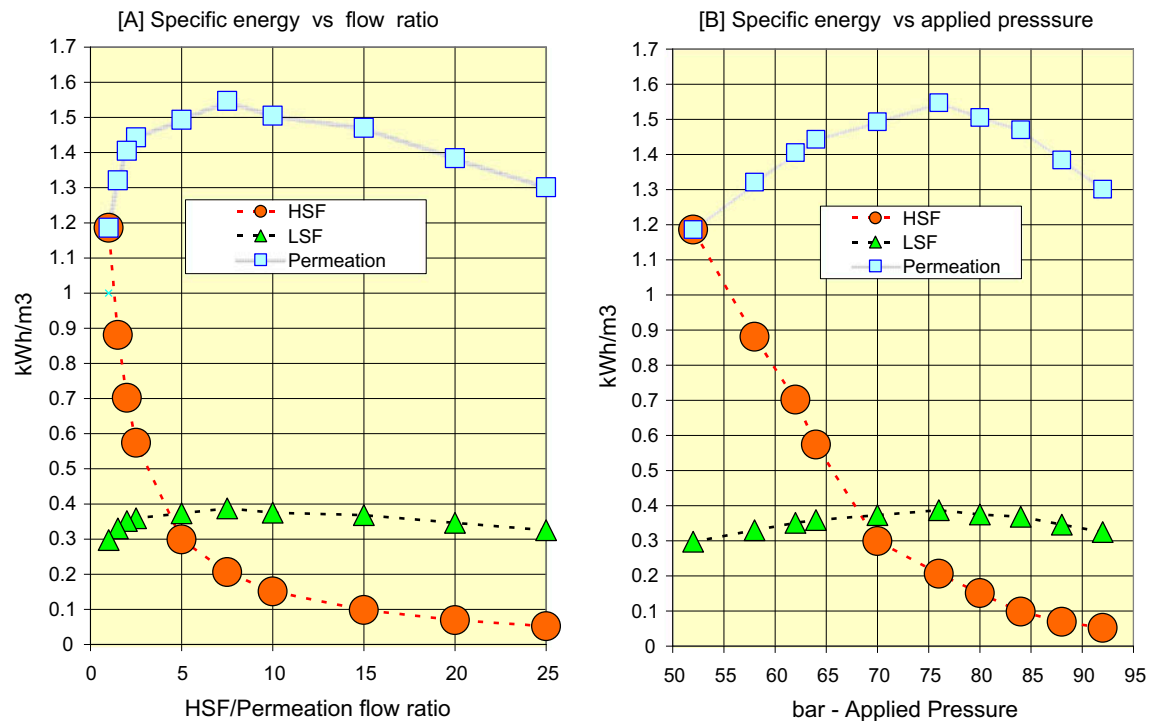


Fig. 7. Specific energy (kWh/m^3) projections based on NEP of HSF, LSF, and permeation flow for SW (4.2%)–SWC (25%) using CC-PRO with HTI-TFC ($A = 2.49 \text{ lmh}$) and $\beta = 0.200$ as function of flow ratio [A] and applied pressure [B].

of the membrane and the information pertaining to power and energy at said limiting pressure is provided in Table 2(B) and Fig. 8. The maximum NEP power availability at the limiting pressure of power availability at the limiting pressure of 39.3 W/m^2 is reached at $\delta = 5.0$ (Fig. 8(A)), instead of 46.2 W/m^2 at $\delta = 7.5$ and 76 bar (Fig. 6) in the absence of pressure restriction. In simple terms, decreased operational pressure by 27.7 bar ($76.0\text{--}48.3 \text{ bar}$) effects only a 15% decline of maximum NEP ($46.2\text{--}39.3 \text{ W/m}^2$). This observation is noteworthy in particular since demonstrates the ability to operate with near maximum NEP output under much relaxed pressure conditions which translate to lower installation costs and operational expenses. It should be pointed out that the NEP projections hereinabove are in the context of the CC-PRO technology and that such data for conventional PRO with ERD are expected to be significantly lower as function of the ERD efficiency and effectiveness.

Power variations under $\delta = 5.0$ and 48.3 bar as function of β in the range $0.18\text{--}0.27$ also explored in order to ascertain the magnitude of such an effect especially since the $\beta = 0.200$ term used in the simulations is said to be a minimum estimate with a realistic range up to 0.22 considered plausible. The simulated data presented in Table 3 and displayed in Fig. 9

reveal the association β of $0.200\text{--}0.22$ with PD of $55.6\text{--}61.2 \text{ W/m}^2$ and NEP of $39.3\text{--}43.2 \text{ W/m}^2$, respectively, which translates to the feasibility of 10% higher power at the limiting pressure of the membrane.

The present state of art prospects for CC-PRO hydroelectric power generation from SW (4.2%)–SWC (25%) with HTI-TFC ($A = 2.49 \text{ lmh/bar}$ and $\beta = 0.200$) under $\delta = 5.0$ at 48.3 bar applied pressure are illustrated in Table 3 and amount to a maximum NEP of 39.3 W/m^2 or 39.3 kW per $1,000 \text{ m}^2$ membrane surface for continuous power generation of 943 kWh/d clean energy sufficient for seawater desalination of $377 \text{ m}^3/\text{d}$ by the energy saving SWRO-CCD technology [46–48]. Assessment of clean energy technologies should be made on the basis of energy production (e.g. kWh/d) due to the large power variations experienced with most natural energy sources (e.g. solar and wind). In contrast with solar and wind energy techniques for clean power generation, CC-PRO enables continuous energy generation of fixed power of high availability irrespective of outdoor conditions (e.g. sun/rain; light/dark; wind velocity; temperature; etc.) provided that the salinity gradient feed solutions (HSF and LSF) are not exhausted. The NEP = 39.3 W/m^2 demonstrated in Table 3 is already well above the

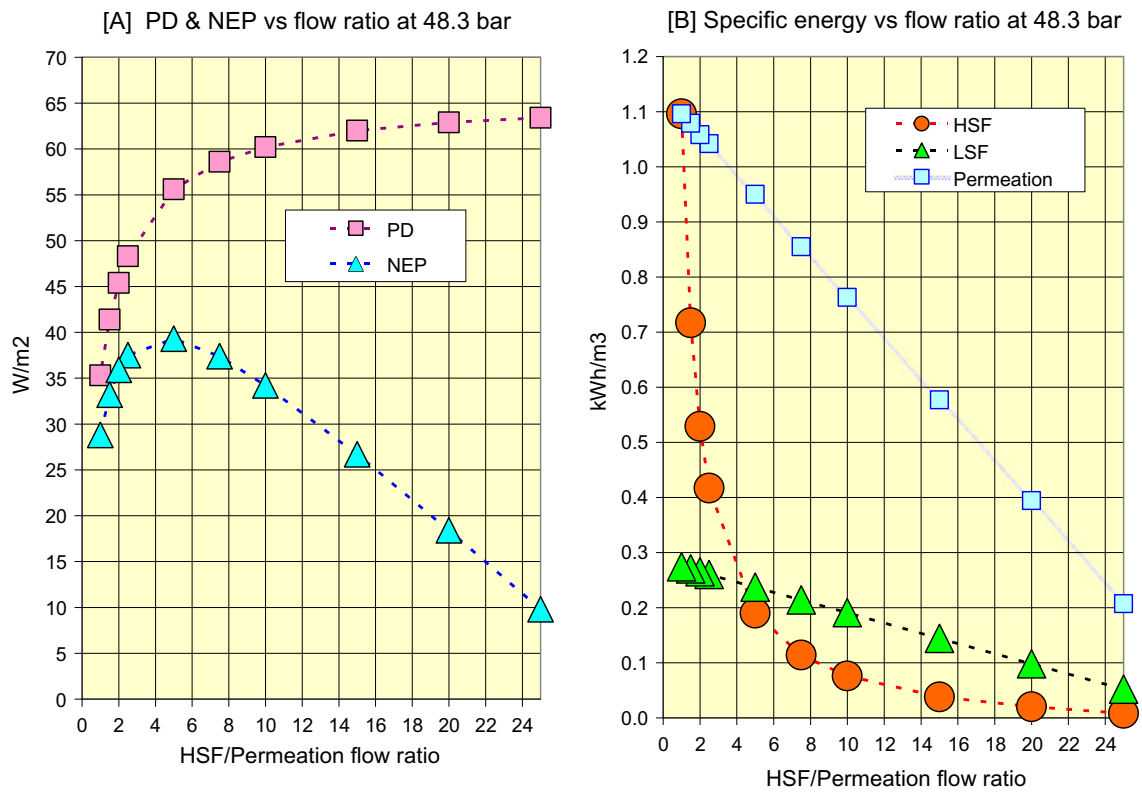


Fig. 8. HSF/Permeation flow ratio relationships to power [A] and specific energy of HSF, LSF, and permeation based on NEP [B] for SW (4.2%)–SWC (25%) using CC-PRO with HTI-TFC ($A = 2.49$ lmh) and $\beta = 0.200$ at an applied pressure of 48.3 bar.

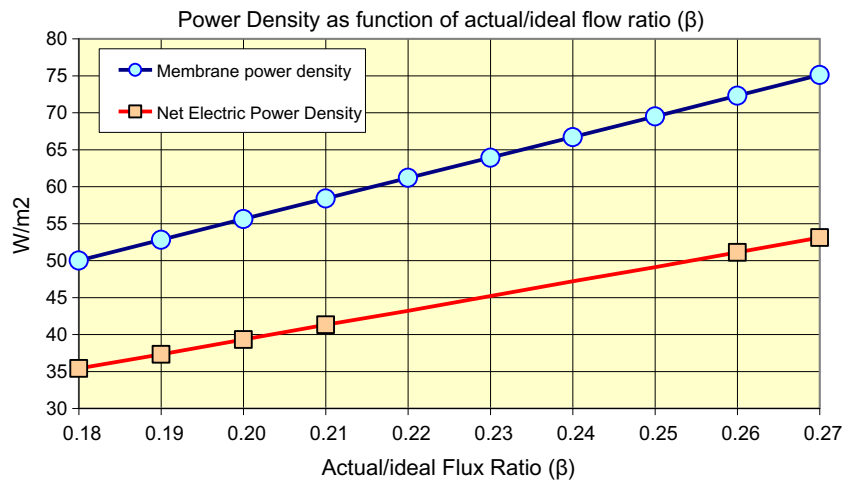


Fig. 9. Maximum power density availability as a function of actual/ideal flux ratio (β) from SW (4.2%)–SWC (25%) using CC-PRO and HTI-TFC ($A = 2.49$ lmh/bar) membrane, or alike, at maximum operational pressure (48.3 bar) according to database in Table 3.

suggested minimum (5.0 W/m²) [9] of economic feasibility, and the rapid progress on PRO membranes performance over the past several years [7–32]

suggests the near future availability of such membranes with $A > 2.49$ lmh/bar and $\beta > 0.200$ for maximum applied pressure greater than 48.3 bar with

NEP > 39.3 W/m², or even NEP >> 39.3 W/m², of enormous economic prospects.

Salinity gradient system of seawater and its desired concentrate (SW–SWC) for CC-PRO power generation application is made of an unlimited LSF source (SW) with supply of HSF (SWC) received from evaporation ponds and/or reservoirs. Reservoirs of HSF can be created on land or in sea adjacent to the coastlines and reach their desired concentration by a natural evaporation process. The salinity of the HSF reservoir in conjunction with CC-PRO is expected to remain unchanged if the average daily evaporation matches the permeation flow rate of CC-PRO. The evaporation rate of the reservoir will depend on its surface area and climate conditions such as temperature, duration of daily solar radiation, wind velocity frequencies, and relative humidity. Accelerated evaporation of HSDF received from the CC-PRO unit prior to entry into the reservoir can be achieved by means of evaporation towers, or shallow ponds, of expanded solar radiation absorbing surfaces exposed to air flow created by wind or induced by fans. Incidentally, the increased air humidity expected in the vicinity of said accelerated HSDF evaporation systems could be exploited in the context of advanced air to water machines, many of which are already commercially available. Moreover, high humidity micro climate created around the proposed evaporation systems, ponds, and reservoirs in desert zones could induce the development of local agriculture, otherwise impossible under normal desert conditions. In order to sustain continuous non-stop power generation by the CC-PRO unit, its reservoir system should experience small daily concentration variations, and since the salt content of the reservoir system remains unchanged, this requirement implies a small daily volume difference (ΔV) between day and night in the reservoir which translates to small concentration variations under 0.05% in the HSF reservoir made of SWC.

Freshwater sources constitute less than 1.0% of the water on earth with most of remaining (99%) exist in the form of seawater with BW account for negligible amounts. Increased reliance on SWRO for freshwater supplies in various parts of the world is imminent in light of the rapidly expanding global population, higher standard of living, declined availability of freshwater sources due to climate changes inflicted by the global “green-house effect”, and increased pollution of ground and surface water. Accordingly, maximizing freshwater production by BWRO from BW sources when available and from clean domestic effluents is of high priority due to the much lower energy costs and operational expenses compared with SWRO. The aforementioned considerations imply that

the use of freshwater and/or clean domestic effluents and/or BW for PRO power generation applications is unwise since such water sources could be used more effectively either directly or after simple regeneration processes (e.g. MF, RO, etc.) to supplement the growing demand for freshwater supplies already evident in various parts of the world. Even where rivers’ outlets to sea can be used for PRO power generation without impeding on freshwater supplies to nearby communities, this approach is of low economical feasibility in the light of the expected small power density of such gradients which imply high installation costs and operational expenses of low power generation prospects as already revealed by the *Statkraft* demonstration plant in Norway [33–35], which was recently discontinued. PRO power generation from clean domestic effluents and brines of seawater desalination plants, such as explored in the Japanese “mega-ton” project [36–38], is also of doubtful economic feasibility since such effluents can be converted to high quality freshwater by inexpensive high recovery low energy BWRO processes which are practiced already on large scale in the “NEWater” plants in Singapore [48] and in Orange District [49] (California, USA). PRO hydroelectric power generation techniques in order to become economically effective require sufficiently high salinity gradients which could be created from seawater (SW = LSF) and its desired concentrate (SWC-HSF) and apply successfully for large-scale clean energy generation in coastlines found in arid regions on earth. The present model study explores the power generation prospects of one such a salinity gradient [SW (4.2%)–SWC (25%)] with the CC-PRO technology [39–41] and the HTI-TFC membrane [44] of the highest documented [32] operational applied pressure (48.3 bar) and reveals the ability to reach high NEP output of clear economical feasibility already on the basis of existing knowledge with new membranes of higher β and applied pressure of operation expected to allow an even greater clean power generation from said salinity gradient in the future.

The concept of SW–SWC salinity gradient for CC-PRO hydroelectric power generation should be applicable in coastal regions worldwide where climate conditions (e.g. solar radiation, temperature, wind, and humidity) allow effective evaporation of reservoirs with seawater concentrates. Seawater evaporation ponds have been used worldwide including North America for NaCl production, and such existing ponds could also apply for clean energy generation by CC-PRO as an added benefit. Countries with long coastal lines in arid zones will benefit the most from the CC-PRO power generation concept of SW–SWC and a partial list of such countries includes, for

example, Saudi Arabia, Yemen, Oman, United Arab Emirate, Sudan, Egypt, Libya, Western Sahara, Mauritania, Australia, Peru, and Chile. The climate conditions along the Red Sea coastlines in Saudi Arabia, Egypt, and Sudan makes these countries probably the best sites for large-scale CC-PRO clean power generation and Kingdom of Saudi Arabia which relies heavily on SWRO desalination for its freshwater supplies could become self-sufficient with clean energy drawn from the seawater. Apart from the aforementioned, many other countries with short coastlines along or near arid zones may have suitable sites for large-scale CC-PRO hydroelectric energy generation.

In contrast with interruptions encountered with solar (e.g. day–night) and wind (e.g. insufficient minimum velocity) power generation techniques, the SWC reservoir of the SW–SWC CC-PRO technology serves as power storage to assure continuous supply of HSF for uninterrupted sustainable power generation. The power storage capacity of the HSF reservoir system depends on its dimensions and location, and with an appropriate design could enable continuous CC-PRO operation over days, or even weeks, of low evaporation periods. In general, the reservoir system should be kept at a salinity level greater than that of the designed CC-PRO process with desired HSF concentration at inlet to unit achieved by blending with seawater or with SWC from a second reservoir of lower salinity. Land-penetrated sea enclaves could be made into reservoirs by dikes, and shoreline reservoir do not require seal since ground water on the beach mainly comprise seawater. The aforementioned implies low investment costs to create SWC reservoirs and low maintenance expenses thereafter. Incidentally, creation of large SWC reservoirs for CC-PRO hydroelectric power generation would require only a small fraction of the investment needs for conventional hydroelectric systems with large reservoirs and dams.

Disregarding reservoirs' aspects, reasonable installation cost of CC-PRO power plants without need of ERD could be estimated on the basis of 35% of the total arising from membranes at a rate of 20 \$/m² or 57,143 \$ per plant with 1,000 m² membrane surface. This estimate considered in the context of existing seawater evaporation ponds of salt production factories and a CC-PRO unit design with HTI-TFC ($A = 2.49$ lmh/bar and $\beta = 0.200$) membranes of 1,000 m² surface area for SW (4.2%)–SWC (25%) operation under $\delta = 5.0$ at 48.3 bar applied pressure according to the data in Table 3 implies 39.3 kW continuous power generation with a specific installation cost of 1,454 \$/kW for an annual energy output of 344,268 kWh. Cost analysis of said CC-PRO unit of 1,000 m² membrane surface assuming 2.0 cent/kWh operation and maintenance

(O&M) costs, 5.0% annual interest rates, and 15% profits on revenues reveals an investment return period of 10 years per 4.9 cent/kWh electricity sold to clients. A 10-fold larger CC-PRO unit of 10,000 m² membrane surface area of the same assumed specific installation cost (1.454 \$/kW) of lower O&M (1.0 instead of 2.0 cent/kWh), interest rates (2% instead of 5%), and profits on revenues (10% instead of 15%) yields an investment return period of five years per 5.0 cent/kWh clean electricity sold to clients. Increased power output expected of future developed PRO-TFC membranes of higher permeability coefficient ($A > 2.49$ lmh/bar) and $\beta > 0.200$ for operational pressure greater than 47.3 bar should result in specific installation costs under 1,000 \$/kW and manifest shorter investment return periods (<5 years) of lower rates (<5.0 cent/kWh) of sold clean electricity to clients.

7. Concluding remarks and summary

This study explores the prospects for clean energy generation in coastal regions from salinity gradient made of SW and its concentrates SWC by the CC-PRO technology of near absolute energy efficiency without ERD and semi-permeable membranes such as HTI-TFC ($A = 2.49$ lmh/bar, $B = 0.39$ lmh, and $S = 564$ μm) of 48.3 bar maximum applied pressure and alike. This power generation process is fueled by SW as low salinity feed (LSF) and SWC as HSF, and the regeneration of HSF from the HSDF can be achieved through evaporation ponds of the types extensively used by the sea salt manufacturing industry. Large-scale harvesting of clean energy from the sea could be found particularly attractive along coastlines of arid zones where climate conditions (e.g. solar radiation, temperature, wind, humidity, etc.) favor effective evaporation from reservoirs of SWC.

The feasibility of seawater as clean power source is ascertained in the current study by theoretical model CC-PRO power simulations of the SW (4.2%)–SWC (25%) salinity gradient with the cited HTI-TFC membrane of actual/ideal flux ratio ($\beta = 0.200$) performance characteristics estimated from relevant FO experimental data in NaCl solutions under different HSF/permeation flow ratio (δ : 1–25) conditions. The results of the simulations reveal membrane peak power density (PD) of 63.1 W/m² at 76 bar with $\delta = 7.5$ and net electric power (NEP) density of 46.2 W/m² which takes account of the efficiency of the turbine generator and the power consumption of auxiliary pumps. Maximum power prospects of PD = 55.6 W/m² and NEP = 39.3 W/m² are revealed under the limiting applied pressure (48.3 bar) of said membrane at $\delta = 5.0$. The aforementioned results suggest the economic

feasibility of seawater utilization for continuous clean power generation in the context of CC-PRO already with existing membranes such as HTI-TFC. Moreover, improved membranes of higher actual/ideal flux ratio ($\beta > 0.200$) and higher applied pressure of operation (> 48.3 bar) expected in the future will enable greater power output per defined membrane surface area, and thereby decrease specific installation cost of CC-PRO units and enhance their economic prospects for low-cost clean energy generation from SW–SWC gradients of greater osmotic pressure differences.

Creation of large HSF/HSDF evaporation reservoirs along coastline of arid zones should enable continuous large-scale clean energy generation day and night independent of climate changes with rather small variations of HSF salinity depending on the size of the reservoirs system wherein power is stored in the context of CC-PRO. Seawater covers most of the surface of our planet and accounts for ~99% of its water content and therefore, the exploitation of this enormous resource for clean energy generation by CC-PRO and for freshwater production by SWRO desalination becomes inevitable in light of the adverse green-house effect on the environmental and the rapidly expanding global population. The exploitation seawater for clean energy generation through CC-PRO according to the present study appears of high economic feasibility if practiced on coastlines along arid zones.

Acknowledgment

Support by Osmotech Ltd Israel is gratefully acknowledged.

References

- [1] S. Loeb, Method and apparatus for generating power utilizing pressure-retarded-osmosis, US patent No 3,906,250, 1975.
- [2] S. Loeb, R.S. Norman, Osmotic-power plants, *Science* 189 (1975) 654–655.
- [3] S. Loeb, Production of energy from concentrated brines by pressure-retarded osmosis, *J. Membr. Sci.* 1 (1976) 49–63.
- [4] S. Loeb, F. van Hessen, D. Shahaf, Production of energy from concentrated brines by pressure-retarded osmosis, *J. Membr. Sci.* 1 (1976) 249–269.
- [5] S. Loeb, Energy production at the Dead Sea by pressure-retarded osmosis: Challenge or chimera? *Desalination* 120 (1998) 247–262.
- [6] S. Loeb, S. Sourirajan, *American Chemical Society Advances in Chemistry Series* 38, ACS, 1963, pp. 117–132.
- [7] A. Achilli, T.Y. Cath, A.E. Childress, Power generation with pressure retarded osmosis: An experimental and theoretical investigation, *J. Membr. Sci.* 343 (2009) 42–52.
- [8] A. Achilli, T.Y. Cath, A.E. Childress, Selection of inorganic-based draw solutions for forward osmosis applications, *J. Membr. Sci.* 364 (2010) 233–241.
- [9] A. Achilli, A.E. Childress, Pressure retarded osmosis: From the vision of Sidney Loeb to the first prototype installation—Review, *Desalination* 261 (2010) 205–211.
- [10] M. Elimelech, W.A. Phillip, The future of seawater desalination: Energy, technology, and the environment, *Science* 333 (2011) 712–717.
- [11] B.E. Logan, M. Elimelech, Membrane-based processes for sustainable power generation using water, *Nature* 488 (2012) 313–319.
- [12] S.J. Duranceau, Emergence of forward osmosis and pressure retarded osmosis process for drinking water treatment, *Florida, Water Resour. J.* July (2012) 32–33.
- [13] X. Wang, Z. Huang, L. Li, S. Huang, E.H. Yu, K. Scott, Energy generation from osmotic pressure difference between the low and high salinity water by pressure retarded osmosis, *J. Technol. Innov. Renew. Energy* 1 (2012) 122–130.
- [14] T.-S. Chung, X. Li, R.C. Ong, Q. Ge, H. Wang, G. Han, Emerging forward osmosis (FO) technologies and challenges ahead for clean water and clean energy applications, *Curr. Opin. Chem. Eng.* 1 (2012) 246–257.
- [15] L. Chekli, S. Phuntsho, H.K. Shon, S. Vigneswaran, J. Kandasamy, A. Chanan, A review of draw solutes in forward osmosis process and their use in modern applications, *Desalin. Water Treat.* 43 (2012) 167–184.
- [16] I.L. Alsvik, M.-B. Hägg, Pressure retarded osmosis and forward osmosis membranes: Materials and methods, *Polymers* 5 (2013) 303–327.
- [17] F. Dinger, T. Tröndle, U. Platt, Optimization of the energy output of osmotic power plants, *J. Renewable Energy*, Article ID 496768, (2013) 7 p. Available from: <http://dx.doi.org/10.1155/2013/496768>.
- [18] C. Klaysom, T.Y. Cath, T. Depuydt, I.F.J. Vankelecom, Forward and pressure retarded osmosis: Potential solutions for global challenges in energy and water supply, *Chem. Soc. Rev.* 42 (2013) 6959–6989.
- [19] M. Sabah, A.F. Atwan, H.B. Mahood, A. Sahrif, Power generation based on pressure retarded osmosis: A design and an optimization study, *Int. J. Appl. Eng. Manage.* 2 (12) (2013) 68–74.
- [20] J.R. McCutcheon, M. Elimelech, Influence of membrane support layer hydrophobicity on water flux in osmotically driven membrane processes, *J. Membr. Sci.* 318 (2008) 458–466.
- [21] N.Y. Yip, A. Tiraferri, W.A. Phillip, J.D. Schiffman, M. Elimelech, Performance thin-film composite forward osmosis membrane, *Environ. Sci. Technol.* 44 (2010) 3812–3818.
- [22] N.Y. Yip, M. Elimelech, Performance limiting effects in power generation from salinity gradients by pressure retarded osmosis, *Environ. Sci. Technol.* 45 (2011) 10273–10282.
- [23] N.Y. Yip, A. Tiraferri, W.A. Phillip, J.D. Schiffman, L.A. Hoover, Y.C. Kim, M. Elimelech, Thin-film composite pressure retarded osmosis membranes for sustainable power generation from salinity gradients, *Environ. Sci. Technol.* 45 (2011) 4360–4369.
- [24] N.Y. Yip, M. Elimelech, Thermodynamic and energy efficiency analysis of power generation from natural salinity gradients by pressure retarded osmosis, *Environ. Sci. Technol.* 46 (2012) 5230–5239.

- [25] S. Chou, R. Wang, L. Shi, Q. She, C. Tang, A.G. Fane, Thin-film composite hollow fiber membranes for pressure retarded osmosis (PRO) process with high power density, *J. Membr. Sci.* 389 (2012) 25–33.
- [26] S. Zhang, T.S. Chung, Minimizing the instant and accumulative effects of salt permeability to sustain ultrahigh osmotic power density, *Environ. Sci. Technol.* 47 (2013) 10085–10092.
- [27] S. Zhang, F. Fu, T.S. Chung, Substrate modifications and alcohol treatment on thin film composite membranes for osmotic power, *Chem. Eng. Sci.* 87 (2013) 40–50.
- [28] X. Li, S. Zhang, F. Fu, T.S. Chung, Deformation and reinforcement of thin-film composite (TFC) polyamide-imide (PAI) membranes for osmotic power generation, *J. Membr. Sci.* 434 (2013) 204–217.
- [29] G. Han, S. Zhang, X. Li, T.S. Chung, High performance thin film composite pressure retarded osmosis (PRO) membranes for renewable salinity—Gradient energy generation, *J. Membr. Sci.* 440 (2013) 108–121.
- [30] X. Song, Z. Liu, D.D. Sun, Energy recovery from concentrated seawater brine by thin-film nanofiber composite pressure retarded osmosis membranes with high power density, *Energy Environ. Sci.* 6 (2013) 1199–1210.
- [31] A.P. Straub, N.Y. Yip, M. Elimelech, Raising the bar: Increased hydraulic pressure allows unprecedented high power densities in pressure-retarded osmosis, *Environ. Sci. Technol. Lett.* 1(1) (2014) 55–59.
- [32] S.E. Skillhagen, J.E. Dugstad, R.J. Aaberg, Osmotic power—Power production based on the osmotic pressure difference between waters with varying salt gradients, *Desalination* 220 (2008) 476–482.
- [33] S.E. Skillhagen, G. Brekke, W.K. Nielsen, Progress in the development of osmotic power, in: *Proceedings. Qingdao International Conference on Desalination and Water Reuse, Qingdao, China, June 20–23, 2011*, pp. 247–260.
- [34] G. Brekke, Review of experience with the Statkraft prototype plant, in: *The 3rd Osmosis Membrane Summit, Barcelona, Spain, April 26–27, 2012*.
- [35] A. Tanioka, Power generation by pressure retarded osmosis using concentrated brine from seawater desalination system and treated sewage, review of experience with pilot in Japan, in: *The 3rd Osmosis Membrane Summit, Barcelona, Spain, April 26–27, 2012*.
- [36] M. Kurihara, Government funded programs worldwide, the Japanese “Mega-ton Water System” project, *The 3rd Osmosis Membrane Summit, Barcelona, Spain, April 26–27, 2012*.
- [37] K. Saito, M. Irie, S. Zaitso, H. Sakai, H. Hayashi, A. Tanioka, Power generation with salinity gradient by pressure retarded osmosis using concentrated brine from SWRO system and treated sewage as pure water, *Desalin. Water Treat.* 41 (2012) 114–121.
- [38] PCT Patent Application, Power generation by pressure retarded osmosis in closed circuit without need of energy recovery, International Publication Number WO 2012/140659 A1, October 18, 2012, inventor—A. Efraty.
- [39] A. Efraty, Closed circuit pressure retarded osmosis—A new technology for clean power generation without need of energy recovery, in: *The 3rd Osmosis Membrane Summit, Barcelona, Spain, April 26–27, 2012*.
- [40] A. Efraty, Pressure-retarded osmosis in closed circuit: A new technology for clean power generation without need of energy recovery, *Desalin. Water Treat.* 51 (2013) 7420–7430.
- [41] A. Hermoni, Actual energy consumption and water cost for the SWRO systems at Palmachim—Case history, IDA conference, CA, USA, November 2–3, 2010.
- [42] A. Efraty, Closed circuit desalination series no-6: Conventional RO compared with the conceptually different new closed circuit desalination technology, *Desalin. Water Treat.* 41 (2012) 279–295.
- [43] <http://www.htisater/>—Hydration Technology Innovations, HTI, Albany, NY.
- [44] A. Efraty, Closed Circuit PRO Series No 2: Performance projections for PRO membranes by a simple approach base on actual/ideal flux ratio at zero applied pressure, *Desalin. Water Treat.* (2015), doi: 10.1080/19443994.2015.1010275.
- [45] A. Efraty, Closed circuit desalination—A new low energy high recovery technology without energy recovery, *Desalin. Water Treat.* 31 (2011) 95–101.
- [46] A. Efraty, R.N.I. Barak, Z. Gal, Closed circuit desalination series no-2: New affordable technology for sea water desalination of low energy and high flux using short modules without need of energy recovery, *Desalin. Water Treat.* 42 (2012) 189–196.
- [47] A. Efraty, Closed circuit desalination series no. 8: Record saving of RO energy by SWRO-CCD without need of energy recovery, *Desalin. Water Treat.* 52(31–33) (2014) 5717–5730.
- [48] Information on “NEWater” production in Singapore. Available from: <http://pub.gov.sg/water/newater>.
- [49] Information on the GWRS program in West Orange District, CA. Available from: <http://www.gwrssystem.com>.